

2023-07

Occurrence and characteristics of fibreglass-reinforced plastics and microplastics on a beach impacted by abandoned fishing boats: A case study from Chellanam, India

Lekshmi, NM

<https://pearl.plymouth.ac.uk/handle/10026.1/21165>

10.1016/j.marpolbul.2023.114980

Marine Pollution Bulletin

Elsevier BV

All content in PEARL is protected by copyright law. Author manuscripts are made available in accordance with publisher policies. Please cite only the published version using the details provided on the item record or document. In the absence of an open licence (e.g. Creative Commons), permissions for further reuse of content should be sought from the publisher or author.

1 **Occurrence and characteristics of fibreglass-reinforced plastics and**
2 **microplastics on a beach impacted by abandoned fishing boats: A**
3 **case study from Chellanam, India**

4

5 N. Manju Lekshmi¹, Sreejith S Kumar¹, P. Muhamed Ashraf¹, S.P. Nehala¹ and Leela Edwin¹,
6 Andrew Turner²

7 1) ICAR-Central Institute of Fisheries Technology, P. O. Matsyapuri, Willingdon Island,
8 Cochin – 682029, India

9 2) School of Geography, Earth and Environmental Sciences, University of Plymouth,
10 Plymouth PL4 8AA, UK

11 *Correspondence: manjulekshmi.n@icar.gov.in / manjuaem@gmail.com (Manju Lekshmi N.)

12

13 <https://doi.org/10.1016/j.marpolbul.2023.114980>

14

15 **Accepted 20 April 2023**

16 **Abstract**

17 Plastics and microplastics have been quantified and characterised at boat disposal sites and
18 along the high-water line (HWL) of a fish landing centre beach in Chellanam, India. Fibreglass-
19 reinforced plastic (FRP) made a greater contribution to the plastic pool at the disposal sites (~
20 4.5 $n\ m^{-2}$ and 18 $g\ m^{-2}$) than at the HWL (~ 0.25 $n\ m^{-2}$ and < 1 $g\ m^{-2}$) and was an abundant
21 component of the microplastic pool at the former. Infrared analysis of microplastic-sized FRPs
22 revealed various resins (e.g., alkyd, polyester, epoxy), while X-ray fluorescence analysis of
23 the painted surfaces of meso-sized FRPs returned variable concentrations of copper and lead.
24 Concentrations of Pb were high enough to contaminate sand up to ~400 $mg\ kg^{-1}$. The relatively
25 high density of FRP and its association with glass fibres and metal-bearing paints results in
26 particles with potentially very different fates and toxicities to more “conventional” (non-
27 composite) thermoplastics.

28

29

30 **Keywords**

31 Debris; fragments; paint; copper; lead; disposal

32

33 **Highlights**

34 Little information exists on fibreglass-reinforced plastic (FRP) as marine litter

35 Different sizes of FRP were found on a beach impacted by fishing boat abandonment

36 FRP can make an important contribution to the microplastic pool

37 Lead in painted surfaces of FRP are sufficient to significantly contaminate sand

38 FRP requires further study because of its association with glass fibres and metals

39 **1. Introduction**

40 Plastic is a versatile, lightweight, chemically stable and inexpensive material with multiple
41 uses across a wide range of sectors. Because of these properties, however, and despite the
42 recyclability of many polymers, the use of plastics, and in particular in the consumer sector,
43 results in the generation of large quantities of poorly-degradable waste. Inadequate
44 management of this waste then leads to contamination of the environment, with the marine
45 setting an ultimate receptor of much plastic (Auta et al., 2017; Woods et al., 2021).

46 In the marine environment, the focus of most research has been on plastic litter along
47 shorelines, and microplastics (with sizes < 5 mm) within intertidal sediments and suspended
48 in the water column. Here, most commonly documented are thermoplastics like polyethene,
49 polypropylene, polyethylene terephthalate and polystyrene (Erni-Cassola et al., 2019).

50 Interest in these polymers is driven by their ubiquity in consumer goods and, for
51 microplastics, constraints on plastic separation from sediments by flotation. The latter
52 normally involves separation of microplastics from other particulate matter in a saturated salt
53 solution whose density typically ranges from 1.2 to 1.8 g cm⁻³ (Mattsson et al., 2022). As a
54 consequence of this approach, however, composite materials whose densities exceed this
55 range, including fibreglass reinforced plastic (FRP), are overlooked.

56 FRP consists of a polymeric matrix or binding agent, such as epoxy or polyester thermoset,
57 that is reinforced with filaments or fibres of textile-grade glass to create a relatively strong
58 and elastic composite. Because of its low cost, low weight and resistance to corrosion, FRP
59 has extensive usage in components and structures in the maritime sector. Of particular
60 importance here is the manufacture of small boats (e.g., fishing boats and recreational craft),
61 with about 80% of vessel hulls up to 20 m in length constructed of FRP (Rubino et al., 2020).
62 In India, FRP is used to construct boat hulls or as a sheathing material over a wooden
63 substrate. Due to the high costs involved in their proper disposal and difficulties in recycling
64 thermosetting composites, however, end-of-life boats constructed of or sheathed by FRP are
65 often abandoned in the coastal zone (Eklund et al., 2013; IMO, 2019).

66 Despite the importance of FRP as a material and contaminant, it has received little attention
67 in the marine environmental literature, with reports limited to its detection in surface trawls
68 (Song et al., 2014; Higgins and Turner, 2023) and the potential toxicity of ground composites
69 to two aquatic organisms (Ciocan et al., 2020). In this study, therefore, we quantified the
70 occurrence within different size fractions of plastic litter on a sandy beach impacted by the
71 FRP-sheathed boats used in the artisanal fishing industry of Chellanam (India). Here, the
72 beach is used as a landing stage and boats are stored, maintained and abandoned without
73 any regulation or guidelines (Lekshmi et al., 2023). FRP particles are characterised

74 microscopically and by infrared spectroscopy, and the content of potentially toxic metals on
75 any painted surfaces is quantified by X-ray fluorescence spectrometry. Local metal
76 contamination by painted FRP is also evaluated by chemical analysis of beach sand.

77

78

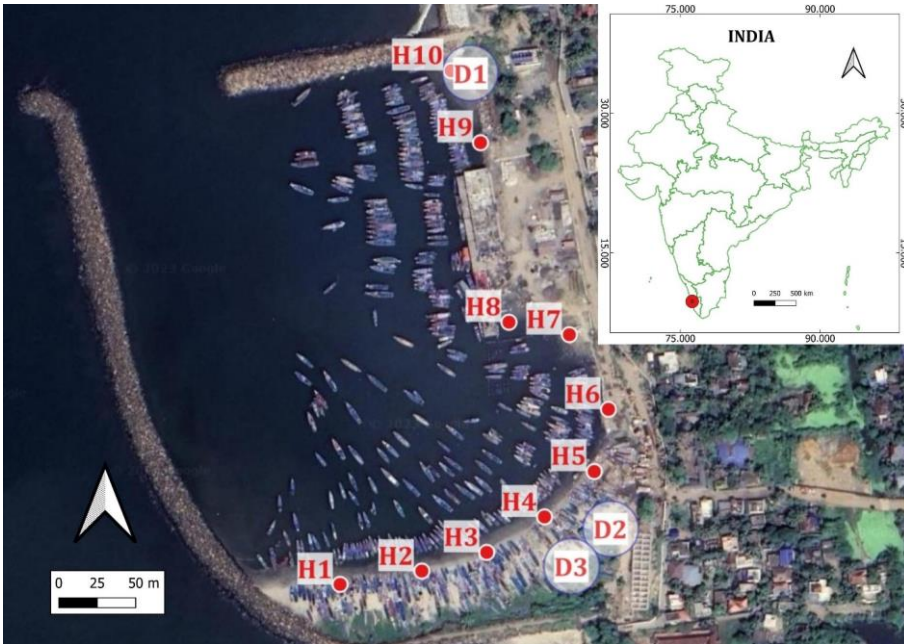
79 **2. Materials and methods**

80 **2.1. Study site and boat abandonment**

81 Chellanam is one of the major small-scale fish landing centres in the Ernakulum district of
82 Kerala. Sampling was undertaken at the landing stage during November 2021 (Figure 1). Most
83 fishing boats operating from Chellanam are motorised and below 14 m in length and are FRP-
84 sheathed over plywood/wood. The life span of these boats is up to ten years but may be
85 significantly shortened by bad weather and rough seas. With no formal decommissioning or
86 disposal process, end-of-life boats are commonly abandoned above the high water line (HWL)
87 on local beaches (Figure 2).

88

89 Figure 1: The location of Chellanam in India and an aerial view of the landing centre.
90 Sampling was undertaken along the HWL from (H1 to H10) and at three disposal sites (D1 to
91 D3).



92
93
94
95
96
97
98
99
100
101
102
103

104

105 Figure 2: The southern reaches of Chellanam landing centre, illustrating the high density of
106 in use and end-of-life boats.

107

108

109

110

111

112

113

114

115

116

117

118

119

120



121

122

123 To quantify fishing boat abandonment, discarded or end-of-life vessels (often inverted and free
124 of any accessories and with visible damage), were counted, landside and waterside, along a
125 transect of the HWL of the entire landing centre (480 m in total; Figure 1).

126

127 **2.2. Sample collection**

128 With aid of Google maps, the HWL was divided into 5 m sections and ten sections were
129 randomly selected according to Lee et al. (2015) (and shown in Figure 1). Just after high water,
130 these sections were visited and used to define 5 m x 5 m quadrats, centred on the HWL (Opfer
131 et al., 2012). Plastic visible at the surface was manually collected from each quadrat and

132 classified as FRP (relatively brittle and flat fragments, often painted on one side and with visible
133 fibres and remains of a wooden substrate on the other side), fishing waste (including
134 polyurethane foam used as an insulating material, netting, floats and sinkers) and other (e.g.,
135 bottles and bottle tops, food packaging, shoes, toys and other fragments). A 0.5 m x 0.5 m
136 quadrat was then defined towards the centre of each main quadrat and sand to a depth of
137 about 2 cm was collected with a stainless-steel trowel and stored in a stainless-steel container
138 in order to determine microplastics and metals. At each disposal site, three 5 m x 5 m quadrats
139 were sampled for plastic debris before three 0.5 m x 0.5 m quadrats were defined within each
140 larger quadrat and sampled for sand as above.

141

142 **2.3. Sample processing**

143 In the laboratory, classes of plastic were counted and weighed and FRP debris was further
144 classified by size as mega-debris: >10 cm; macro-debris: 2 - 10 cm; and meso-debris: 5 - 20
145 mm (Jayasiri et al., 2013). About 1 kg of sand from each small quadrat along the HWL ($n =$
146 10) and within the disposal sites ($n = 9$) was weighed out on a Sartorius electronic balance
147 before the contents were passed through a 5-mm stainless steel sieve. Material passing
148 through the sieve was dried at 40 °C for 24 h before being subject to density separation. Thus,
149 30 g of material was added to a 100 mL solution of saturated $ZnCl_2$ (CDH Analytical Grade in
150 Milli-Q water) of density 1.6 to 1.7 g cm^{-3} in a glass beaker and the contents were agitated
151 with a magnetic stirrer for 20 min before being allowed to settle for 2 h. Supernatants were
152 filtered through individual Whatman 41 filter papers (20 μm pore size) before retained particles
153 were passed through a sequence of stainless steel sieves (mesh sizes 300 μm and 63 μm) to
154 separate coarse (300 μm to 5 mm), medium (63 μm to 300 μm) and fine (20 μm to 63 μm)
155 material and microplastics. Fractionated particles were transferred to watch glasses and
156 plastic particles identified, counted and categorised (by shape, size and colour) under a LEICA
157 MZ16A stereomicroscope at up to 230 X magnification.

158 **2.4. Microplastic identification by FTIR**

159 The polymer content of selected, fractionated microplastics of various shapes, colours and
160 sizes from the HWL ($n = 13$) and disposal sites ($n = 33$) and ten fragments cut or plucked from
161 abandoned boat hulls was determined by attenuated total reflectance Fourier Transform infra-
162 red (ATR-FTIR) spectroscopy. Specifically, small offcuts with no visible extraneous
163 contamination or paint were placed on the diamond compression cell of a Thermo Scientific
164 ATR sampling accessory and analysed using a Thermo Scientific Nicolet iS 10 spectrometer.

165 Spectra were acquired between 650 and 4000 cm^{-1} , with 50 scans per sample, and were
166 compared with a Hummel polymer library embedded in Omnic software.

167

168 **2.5. Sample digestion and copper and lead analysis**

169 From six sand samples along the HTL and all samples from the disposal sites ($n = 9$), about
170 10 g of < 5 mm material was ground in a pestle and mortar. In triplicate, 1 g portions were
171 weighed into a series of acid-cleaned, 50 mL Pyrex beakers to which 8 mL of aqua-regia (3:1
172 HCl:HNO₃; Merck AR) was added. The contents of each beaker were covered with a watch
173 glass and gently boiled on a hotplate for 1 h before the cooled digests were vacuum-filtered
174 through 0.45 μm Whatman Millipore filters. Filtrates were transferred to volumetric flasks and
175 made up to 50 mL with Milli-Q water pending analysis. Triplicate controls were subject to the
176 same protocol but in the absence of sand.

177 Copper and Pb, as indicators of contamination from boat paints, were analysed in the digests
178 by inductively coupled plasma-optical emission spectroscopy (ICP-OES) using a Perkin Elmer
179 Optima 2000 DV. The instrument was calibrated with blanks and standards of 0.1, 0.2, 0.5
180 and 1 mg L^{-1} prepared from dilutions of a NIST multi-element standard.

181 The Cu and Pb content of the painted surfaces of a range of randomly selected meso-
182 fragments of FRP that had been retrieved from the HWL ($n = 12$) and disposal sites ($n = 17$)
183 were determined by portable X-ray fluorescence (XRF) spectrometry. Specifically, we used a
184 Niton XL3t He GOLDD+ spectrometer housed in a laboratory test and operated in a plastics
185 mode (counting time 30 s) according to procedures detailed elsewhere (Turner and Solman,
186 2016). Precise limits of detection varied depending on sample thickness but were typically
187 around 30 mg kg^{-1} for Cu and 10 mg kg^{-1} for Pb.

188

189

190 **3. Results and Discussion**

191 **3.1. Abandoned boats and plastic debris**

192 Across the entire length of the landing centre, we observed 27 abandoned boats, of which 21
 193 were within disposal sites and six were encountered around the HWL. All abandoned boats
 194 were constructed of plywood sheathed with approximately 6 mm of FRP, and ranged in length
 195 from 6 m to 8 m.

196

197 Table 1: Summary of plastic debris (on a number basis and by size category for FRP)
 198 recovered from the quadrats along the HWL and within the disposal sites. Also shown are the
 199 average numbers of plastic per m² based on totals for each category divided by the total area
 200 of quadrats surveyed.

201

| | FRP | | | fishing | other |
|--------------------------|------|-------|------|---------|-------|
| | mega | macro | meso | | |
| HWL | | | | | |
| H1 | 0 | 0 | 7 | 2 | 5 |
| H2 | 0 | 2 | 0 | 7 | 1 |
| H3 | 1 | 12 | 5 | 5 | 5 |
| H4 | 0 | 0 | 0 | 7 | 7 |
| H5 | 1 | 3 | 0 | 3 | 2 |
| H6 | 0 | 0 | 12 | 3 | 3 |
| H7 | 1 | 0 | 3 | 1 | 4 |
| H8 | 0 | 0 | 7 | 1 | 3 |
| H9 | 0 | 2 | 4 | 6 | 3 |
| H10 | 0 | 1 | 0 | 3 | 2 |
| total | 3 | 20 | 38 | 38 | 35 |
| <i>n</i> m ⁻² | 0.01 | 0.08 | 0.15 | 0.15 | 0.14 |
| disposal sites | | | | | |
| D1 | 8 | 25 | 225 | 37 | 20 |
| D2 | 4 | 101 | 257 | 37 | 16 |
| D3 | 20 | 92 | 289 | 12 | 36 |
| total | 32 | 218 | 771 | 86 | 72 |
| <i>n</i> m ⁻² | 0.14 | 0.97 | 3.43 | 0.38 | 0.32 |

202

203 Table 1 summarises the number of pieces of plastic debris retrieved from the quadrats along
 204 the HWL (H1 to H10) and within the three disposal sites (D1, D2 and D3). Along the HWL, 134
 205 pieces of plastic debris were recovered, of which about 46% were visually identified as FRP.
 206 At the disposal sites 1179 pieces of plastic debris were recovered of which about 87% were

207 FRP. When normalised on an area basis, debris in each category, and in particular for the
208 different size classes of FRP, was greater at the disposal sites than along the HWL.

209 Table 2 summarises the plastic debris data on a mass basis. Along the HWL, over 2 kg of
210 plastic was retrieved, with fishing waste contributing more than 70% and FRP contributing
211 about 5%. By comparison, at the disposal sites more than 11 kg was retrieved, with fishing
212 waste contributing 45% and FRP contributing about 36%.

213

214 Table 2: Summary of plastic debris (on a mass basis and by size category for FRP) recovered
215 from the quadrats along the HWL and within the disposal sites. Also shown are the masses of
216 plastic per m² for each category.

217

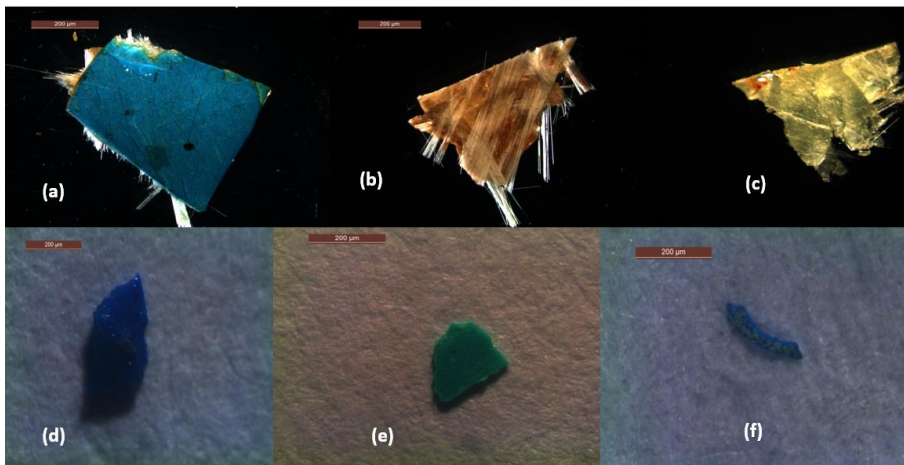
| | FRP | | | fishing | other |
|-------------------|------|-------|------|---------|-------|
| | mega | macro | meso | | |
| HWL | | | | | |
| g | 60 | 30 | 27 | 1530 | 505 |
| g m ⁻² | 0.24 | 0.12 | 0.11 | 6.12 | 2.02 |
| disposal sites | | | | | |
| g | 2160 | 1305 | 480 | 4925 | 2180 |
| g m ⁻² | 9.60 | 5.80 | 2.13 | 21.89 | 9.69 |

218

219

220

221 **3.2. Microplastic abundance and visual characteristics**



222
223 Figure 3: Examples of FRP and other microplastic fragments observed under the
224 microscope. (a) and (b) were taken directly from abandoned boats and (c) to (f) were
225 sampled from disposal sites.

226
227 Microscopic images of six microplastic fragments retrieved in the study are shown in Figure
228 3. Fragments were either (i) relatively stiff and flat irregular shapes, with (often) one or more
229 straight edge and straight fibres in parallel bundles and usually with one painted surface
230 (Figures 3a, 3b and 3c), or (ii) irregular shapes with angular or curved edges and no
231 evidence of fibrous additives or painted surfaces (Figures 3d, 3e and 3f). Microplastic fibres
232 (not illustrated) consisted of single, twisted threads or filaments that were sometimes coiled
233 or single or multiple threads that appeared to be intertwined, while microplastic pellets (not
234 illustrated) were distinctly rounded but with occasional irregularities (e.g., pits, protrusions,
235 overlapping layers).

236 Table 3 shows the number of MPs identified in the quadrats at each location, normalised to a
237 sediment mass of 30 g, along with their distributions by size and shape. Along the HWL,
238 numbers range from 34 to 155 with a median of 82. At the disposal sites, numbers range
239 from 54 to 253 with a median of 127. Overall, and at both the HWL and disposal sites,
240 numbers in the coarse fraction ranged from 21 to 52, while in the medium and fine fractions
241 numbers were more heterogenous between locations, ranging from 2 to 182 and from 5 to
242 72, respectively. Fragments were the most abundant shape in the study and pellets were the
243 least abundant.

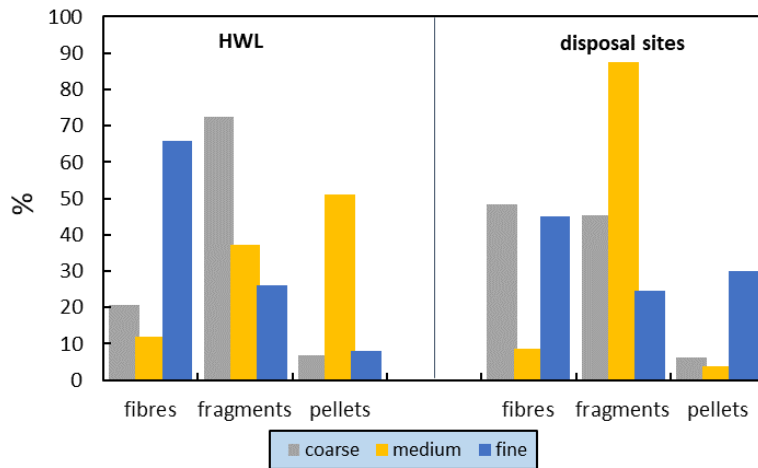
244 On a size basis, however, and as illustrated in Figure 4, the percentage of fragments
245 decreased with decreasing size at the HWL (from about 72% in coarse to about 26% in fine)
246 whereas pellets (about 50%) and fibres (about 65%) were most important in the medium and
247 fine fractions, respectively. By contrast, at the disposal sites, fragments dominated the
248 medium size fraction (nearly 90%) whereas pellets and fibres were most important in the
249 fines.

250 Figure 5 compares the percentages of each microplastic shape by colour along the HWL and
251 at the disposal sites. More abundant along the HWL, and lying below unit slope, are all red
252 microplastics, blue fragments and fibres, yellow and green pellets and fragments, and brown
253 fibres. More abundant at the disposal sites, and above the line of unit slope, are white
254 microplastics, blue pellets, yellow fibres and brown fragments and pellets.

255 In summary, therefore, there were no clear differences in microplastic numbers among the
256 sites and location types, but differences were more evident in size, shape and colour
257 distribution.

258

259 Figure 4: Percentage distribution of microplastics by size and shape across the HWL and at
 260 the disposal sites.

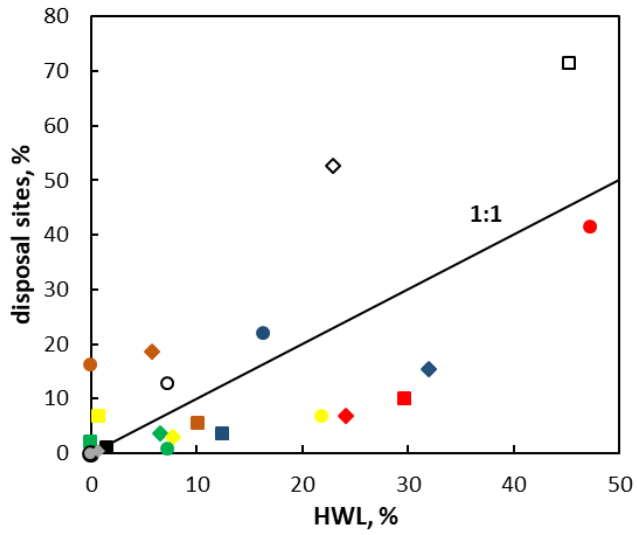


261
 262
 263
 264
 265
 266
 267

Table 3: Number of MPs identified in the quadrats at each location and categorised by size and shape. Note that MPs along the HWL are per 30 g of sediment and those at the disposal sites are totals for three sites each but normalised to a mass of 30 g.

| location | coarse | | | | medium | | | | fine | | | | total |
|----------------|--------|-----------|-------|-----|--------|-----------|-------|-----|--------|-----------|-------|-----|-------|
| | fibres | fragments | beads | sum | fibres | fragments | beads | sum | fibres | fragments | beads | sum | |
| HWL | | | | | | | | | | | | | |
| H1 | 0 | 42 | 10 | 52 | 4 | 11 | 16 | 31 | 31 | 15 | 5 | 51 | 134 |
| H2 | 13 | 17 | 0 | 30 | 1 | 5 | 7 | 13 | 20 | 7 | 1 | 28 | 71 |
| H3 | 4 | 16 | 1 | 21 | 2 | 8 | 10 | 20 | 24 | 14 | 5 | 43 | 84 |
| H4 | 9 | 30 | 0 | 39 | 4 | 18 | 22 | 44 | 56 | 15 | 1 | 72 | 155 |
| H5 | 8 | 36 | 2 | 46 | 0 | 11 | 11 | 22 | 23 | 4 | 0 | 27 | 95 |
| H6 | 9 | 19 | 3 | 31 | 0 | 4 | 4 | 8 | 11 | 12 | 7 | 30 | 69 |
| H7 | 3 | 18 | 0 | 21 | 1 | 0 | 1 | 2 | 4 | 6 | 1 | 11 | 34 |
| H8 | 0 | 18 | 3 | 21 | 4 | 8 | 12 | 24 | 25 | 4 | 3 | 32 | 77 |
| H9 | 14 | 10 | 4 | 28 | 5 | 5 | 10 | 20 | 20 | 7 | 5 | 32 | 80 |
| H10 | 11 | 41 | 0 | 52 | 2 | 2 | 6 | 10 | 14 | 7 | 0 | 21 | 83 |
| disposal sites | | | | | | | | | | | | | |
| D1 | 13 | 18 | 2 | 33 | 3 | 7 | 4 | 15 | 3 | 1 | 1 | 5 | 54 |
| D2 | 18 | 25 | 1 | 44 | 4 | 175 | 3 | 182 | 4 | 8 | 14 | 26 | 253 |
| D3 | 31 | 13 | 5 | 49 | 13 | 22 | 2 | 37 | 25 | 9 | 8 | 42 | 127 |

268



269

270

271 Figure 4: Scatter plot of the percentages of fibres (squares), fragments (diamonds) and
 272 pellets (circles) by colour at the disposal sites and along the HWL (note that transparent is
 273 represented by grey). The line represents unit slope.

274

275 **3.3. Polymeric composition of microplastics**

276 Results of the FTIR analysis of selected samples ($n = 56$) are summarised in Table 4. The
277 ten fragments obtained from abandoned boats were identified as resinous, with alkyd resin
278 most abundant and polyester-, epoxy-, polystyrene- and piperylene-based resins also
279 present. In seven cases, fragments contained glass fibres that were visible under the
280 microscope (e.g., Figure 3) and that were most evident in the FTIR spectra as absorbance
281 peaks in the region $1000-1200\text{ cm}^{-1}$ through asymmetric stretches associated with silicate
282 glass (Hopkinson et al., 2021). At the disposal sites, there was a combination of resin-based
283 fragments with or without visible glass fibres, and non-resinous fragments, fibres and beads
284 that were dominated by polyethylene and polypropylene. Along the HWL, resinous materials
285 were not identified and polyethylene was the most abundant polymer among the various
286 fragments and fibres tested.

287 Table 4: Distribution by polymer type of samples positively identified from abandoned boats,
288 disposal sites and HWL (n represents the total number of samples analysed in each
289 category). Note that polyester includes polyethylene terephthalate.

| | resin | polyolefin | polyester | polyamide |
|-----------------------------|-------|------------|-----------|-----------|
| boats ($n = 10$) | 10 | | | |
| disposal sites ($n = 33$) | 10 | 18 | 1 | |
| HWL ($n = 13$) | | 9 | 2 | 1 |

291

292 **3.4. Copper and lead in sand and mesoplastic FRP**

293 The concentrations of Cu and Pb in sand samples are shown in Table 5. Mean
294 concentrations of Cu range from 1.1 mg kg^{-1} to 11.0 mg kg^{-1} , with relative standard
295 deviations for replicate analyses ranging from about 5% to 35%. Median concentrations are
296 1.5 mg kg^{-1} and 3.6 mg kg^{-1} at the HWL and disposal sites, respectively, with a Mann-
297 Whitney U-test (Minitab, v19) revealing a significantly higher median ($p < 0.05$) at the latter.
298 Mean concentrations of Pb are greater than Cu in each sample and are more variable
299 (ranging from about 3 mg kg^{-1} to 400 mg kg^{-1}). As with Cu, median concentrations are
300 significantly higher at the disposal site than the HWL.

301

302 Concentrations of Cu and Pb in the mesoplastic FRP fragments analysed by XRF are
303 summarised in Table 6. Where detected, Cu concentrations are greater than those found in
304 sand by up to two orders of magnitude but, according to a Mann-Whitney U-test, median

305 concentrations are not significantly different between ($p < 0.05$) the HWL and disposal sites.
306 Lead was detected in fewer mesoplastics but median concentrations are significantly higher
307 than Cu in both the HWL and disposal sites.

308

309

310 Table 5: Concentrations of Cu and Pb (in mg kg⁻¹) in samples of sand from the HWL and
 311 disposal sites. Note that here, individual data are shown for each quadrat (a, b, c) of the
 312 disposal sites. Errors are one standard deviation about the mean of three determinations.

| | Cu | Pb |
|----------------|----------|------------|
| HWL | | |
| H2 | 1.1±0.3 | 7.8±1.0 |
| H3 | 1.6±0.5 | 2.8±0.6 |
| H4 | 1.5±0.2 | 3.9±0.2 |
| H6 | 2.9±0.2 | 6.3±0.1 |
| H9 | 1.5±0.1 | 3.4±0.6 |
| H10 | 7.5±1.1 | 26.5±2.0 |
| median | 1.5 | 5.1 |
| disposal sites | | |
| D1a | 3.1±0.3 | 12.8±2.5 |
| D1b | 6.2±0.5 | 8.0±0.3 |
| D1c | 11.0±1.1 | 50.3±0.8 |
| D2a | 3.3±0.5 | 5.4±1.0 |
| D2b | 3.5±1.3 | 10.5±1.2 |
| D2c | 3.7±0.7 | 58.3±3.5 |
| D3a | 6.2±1.0 | 391.8±35.0 |
| D3b | 3.5±0.4 | 9.7±0.3 |
| D3c | 2.8±0.3 | 7.8±0.1 |
| median | 3.6 | 30.4 |

313

314

315 Table 6: Summary statistics for the concentrations of Cu and Pb (in mg kg⁻¹) in the
 316 mesoplastics sampled from the HWL and disposal sites.

| | Cu | Pb |
|---------------------------------|--------|---------|
| HWL (<i>n</i> = 10) | | |
| no. detected | 8 | 5 |
| median | 304.5 | 752.2 |
| min | 35.7 | 82.6 |
| max | 1047.0 | 1858.0 |
| disposal sites (<i>n</i> = 17) | | |
| no. detected | 16 | 13 |
| median | 118.6 | 345.3 |
| min | 17.7 | 15.0 |
| max | 985.2 | 33606.6 |

317

318 **4. Discussion**

319 The maintenance and abandonment of fishing boats on the beach at Chellanam is
320 associated with high levels of various forms of visible (> 5 mm) plastic waste, both on a
321 number basis and a mass basis and in particular for FRP, compared with the neighbouring
322 HWL. The waste may be generated by the decay and weathering of the boats themselves, or
323 the disposal of other, more general waste at locations of abandonment. As pointed out by
324 Turner and Rees (2016), the presence of discarded boats may be perceived as justification
325 for the deliberate dumping of other forms of litter.

326 Microplastics (< 5 mm) were dominated by similar quantities of fragments at both the
327 disposal sites and along the HWL, but differences were evident between the colour and size
328 distributions at the different location types. Analysis of a selection of microplastics by FTIR
329 revealed a variety of polymers at the disposal sites, including various resins used in FRP, but
330 a dominance of polyolefins at the HWL. This discrepancy maybe related to the lower
331 densities of polyethylene and polypropylene than FRP. Thus, while the density of polyolefins
332 is below 1 g cm⁻³, the density of plastic resins reinforced by glass fibres (often visible under
333 the microscope and confirmed by FTIR) is typically between 1.25 to 2.5 g cm⁻³ (Abbood et
334 al., 2021), with slight modifications possible when the surface is painted. The lower density
335 plastics may be more readily transported from the disposal sites to the HWL and, with
336 buoyant plastics derived from offshore, are subject to redistribution, recirculation and
337 accumulation in the intertidal zone (Graca et al., 2017). Conversely, higher density FRP is
338 less readily transported to the HWL (Ciocan et al., 2020), and any material reaching this area
339 is more likely to be subject to transportation with subsurface offshore currents and sinking
340 and burial.

341 Analysis of the painted surfaces of larger fragments of meso-sized FRP from the disposal
342 sites and, where available, the HWL, indicate variable concentrations of Cu, but at levels
343 insufficient to act as an antifoulant (Singh and Turner, 2009). More significant from an
344 environmental perspective, however, are variable but higher (median) concentrations of Pb.
345 Quantitatively, our results are similar to those reported by Hopkinson et al. (2021) for 14
346 samples of FRP sourced from various breakers yards in southern England (Cu ~ 150 to 1600
347 mg kg⁻¹; Pb ~ 95 to 10,400 mg kg⁻¹). This suggests that, despite extensive restrictions on the
348 Pb content of consumer paints, leaded paint is still used or has been applied relatively
349 recently on FRP more generally. With regard to India, a maximum Pb concentration in
350 consumer paints of 90 mg kg⁻¹ has been required since 2017. However, we note that in a
351 chemical assessment of Indian paints undertaken since the restrictions, Arora et al. (2018)
352 found that paints with very high levels of Pb are still widely sold across the country and that

353 consumer awareness of the problem is extremely low. In the present setting at least, a
354 consequence of the use and removal of leaded paint is that beach sand is heterogeneously
355 contamination by the metal, both within and between disposal sites. Contamination may
356 arise directly from the presence of Pb-rich paint-FRP particulates in the sand, or indirectly via
357 the dissolution of particulate Pb and its adsorption to neighbouring sand grains. Significantly,
358 the Pb concentration in one sample at disposal site D3 exceeded the CCME marine
359 sediment quality guideline for the protection of aquatic life (112 mg kg⁻¹; Canadian Council of
360 Ministers of the Environment, 2012).

361 There is very little information on the occurrence, fate and effects of FRP in the marine
362 science literature, and especially regarding microplastics in sediment, from which to draw
363 comparisons with the present study. The main reason for this is, likely, that conventional
364 means of isolating microplastics from sediments involves flotation in a saturated salt solution,
365 and common solutions employed, like NaCl, NaI and ZnCl₂ (Cutroneo et al., 2021), have a
366 density range (~1.2 to of 1.8 cm⁻³) that would preclude many glass-reinforced resins.
367 Nevertheless, given the importance of FRP in the leisure and commercial boating sectors
368 (Ciocan et al., 2020) and with regard to other maritime structures (Summerscales et al.,
369 2016), and the documentation of other boat-derived debris (mainly paint particles) in the
370 vicinity of boat maintenance facilities or near to abandoned boats (Singh and Turner, 2009;
371 Eklund et al., 2014; Rees et al., 2014; Turner and Rees, 2016; Soroldoni et al., 2018), FRP
372 contamination is predicted to be a more general problem.

373 Unlike sediment, microscopic particles of FRP or the common resins used therein have been
374 reported at the surface of seawater. Specifically, Song et al. (2014) identified polymers
375 originating from paints and FRP used on ships off the southern coast of Korea, while Higgins
376 and Turner (2023) found particles of polyester and epoxy resins in coastal waters around
377 Plymouth, UK. It was suggested that particles were shed from transiting vessels and, despite
378 their relatively high densities, could be maintained temporarily at the sea surface through
379 surface tension or when associated with other floating debris.

380 Despite limited information on the abundance and properties of microscopic FRP particles,
381 they are potentially more hazardous than "conventional" MPs that are commonly described
382 and studied. Thus, in addition to a resinous matrix, FRP is a source of glass fibres that have
383 similar physical and chemical properties to asbestos (Galimany et al., 2009), and harmful
384 leaded pigments in associated paints. In the only study of the ecotoxicological impacts of
385 FRP that we are aware of, Ciocan et al. (2020) exposed fine particles ground from a
386 laminated sheet sourced from a boatyard in southern England (< 4 mm and up to 120 mg L⁻¹)
387 to the mussel, *Mytilus edulis*, and water flea, *Daphnia magna*. In *M. edulis*, FRP was

388 detected in the digestive tubules and gills and caused a range of inflammatory responses in
389 all examined organs. In *D. magna*, particles adhered to the filament hairs of appendages and
390 impaired swimming.

391

392 **5. Conclusions**

393 High concentrations of plastic debris and microplastics have been found on and within the
394 sand in the vicinity of boat disposal sites on the landing stage at Chellanam. Plastic was
395 heterogeneously distributed amongst different sites and between size classifications and
396 colours, but fragments of FRP made a significant and persistent contribution to the litter pool
397 in all cases. By comparison, along the HWL, plastic was less abundant and the contribution
398 from FRP was lower. Paint associated with FRP had variable contents of Cu and Pb, with
399 concentrations of the latter being sufficient to contaminate sediments from a few mg kg⁻¹ up
400 to about 400 mg kg⁻¹. Because of its relatively high density, FRP is generally overlooked in
401 studies of plastics, and in particular microplastics. However, given its association with
402 asbestos-like glass fibres and metal-bearing paints, further environmental studies are
403 recommended.

404

405 **Acknowledgments**

406 The authors thank ICAR for funding the study and the Director of the ICAR-Central Institute
407 of Fisheries Technology for providing facilities and guidance. We are grateful to the
408 fishermen of Chellanam for their time, cooperation and hospitality during the investigation,
409 and the technical staff of the Fishing Technology Division of ICAR-CIFT for their support.

410

411

412

413

414

415

Commented [H1]:

416 **References**

- 417 Abbood, I.S., Odaa, S.A., Hasan, K.F., Jasim, M.A., 2021. Properties evaluation of fiber
418 reinforced polymers and their constituent materials used in structures – A review. *Materials*
419 *Today Proceedings* 43, 100301008.
- 420 Arora, T., Rajankar, P., Chetry, B., 2018. Lead in paints in India: Concerns and Challenges.
421 *Toxics Link*, New Delhi, 48pp.
- 422 Auta, H.S., Emenike, C.U., Fuziah, S.H., 2017. Distribution and importance of microplastics in
423 the marine environment: A review of the sources, fate, effects, and potential solutions.
424 *Environmental International* 102, 165-176.
- 425 Canadian Council of Ministers of the Environment (2012) Canadian Environmental Quality
426 Guidelines and Summary Table: <http://www.ccme.ca/> accessed 12/2022.
- 427 Ciocan, C., Kristova, P., Annels, C., Derjean, M., & Hopkinson, L. (2020). Glass reinforced
428 plastic (GRP) a new emerging contaminant - First evidence of GRP impact on aquatic
429 organisms. *Marine Pollution Bulletin*, 160, 111559.
- 430 Cutroneo, L., Reboa, A., Geneselli, I., Capello, M., 2021. Considerations on salts used for
431 density separation in the extraction of microplastics from sediments. *Marine Pollution Bulletin*
432 16, 112216.
- 433 Eklund, B., Haaksi, H., Syversen, F., Elsted, R., 2013. Norden, (2013). Disposal of End-of-
434 life Plastic Boats. TemaNord [https://www.diva-portal.org/smash/get/](https://www.diva-portal.org/smash/get/diva2:741961/FULLTEXT01.pdf)
435 [diva2:741961/FULLTEXT01.pdf](https://www.diva-portal.org/smash/get/diva2:741961/FULLTEXT01.pdf). Accessed 12/2022.
- 436 Eklund, B., Johansson, L., Ytreberg, E., 2014. Contamination of a boatyard for maintenance
437 of pleasure boats. *Journal of Soils and Sediments* 14, 955-967.
- 438 Erni-Cassola, G., Zadjelovic, V., Gibson, M.I., Christie-Oleza, J.A., 2019. Distribution of plastic
439 polymer types in the marine environment; a meta-analysis. *J. Hazard. Mater.* 369, 691-698.
- 440 GESAMP, 2015. Sources, fate and effects of microplastics in the marine environment: A global
441 assessment. In: Kershaw, P.J. (Ed.), *GESAMP Reports & Studies* 93, International Maritime
442 Organization, London.
- 443 Galimany, E., Ramón, M., Delgado, M., 2009. First evidence of fiberglass ingestion by a
444 marine invertebrate (*Mytilus galloprovincialis* L.) in a NW Mediterranean estuary. *Mar. Pollut.*
445 *Bull.* 58, 1334–1338.

446 Graca, B., Szewc, K., Zakrzewska, D., Dolega, A., Szczerbowska-Boruchowska, M., 2017.
447 Sources and fate of microplastics in marine and beach sediments of the Southern Baltic Sea—
448 a preliminary study. *Environmental Science and Pollution Research* 24, 7650-7661.

449 Higgins, C., Turner, A., 2023. Microplastics in surface waters around Plymouth, UK:
450 Differential sources and transport of fibres and fragments. *Science of the Total Environment*
451 (in review).

452 IMO, 2019. End-of-Life Management of Fibre Reinforced Plastic Vessels: Alternatives to at
453 Sea Disposal. International Maritime Organisation, CPY Group UK.
454 [https://wwwcdn.imo.org/localresources/en/OurWork/Environment/Documents/Fibre%20Reinf](https://wwwcdn.imo.org/localresources/en/OurWork/Environment/Documents/Fibre%20Reinforced%20Plastics%20final%20report.pdf)
455 [orced%20Plastics%20final%20report.pdf](https://wwwcdn.imo.org/localresources/en/OurWork/Environment/Documents/Fibre%20Reinforced%20Plastics%20final%20report.pdf).

456 Jayasiri, H. B., Purushothaman, C. S., & Vennila, A., 2013. Quantitative analysis of plastic
457 debris on recreational beaches in Mumbai, India. *Marine Pollution Bulletin* 77, 107–112.

458 Lee, J., Lee, J. S., Jang, Y. C., Hong, S. Y., Shim, W. J., Song, Y. K., Hong, S. H., Jang, M.,
459 Han, G. M., Kang, D., 2015. Distribution and size relationships of plastic marine debris on
460 beaches in South Korea. *Archives of Environmental Contamination and Toxicology* 69, 288–
461 298.

462 Lekshmi, N.M., Kumar, S.S., Ashraf, P.M., Xavier, K.A.M., Prathish, K.P., Ajay, S.V., Edwin,
463 L., Turner, A., 2023. Abandonment of fibreglass reinforced plastic fishing boats in Kerala, India,
464 and chemical emissions arising from their burning. *Estuarine, Coastal and Shelf Science*
465 (submitted).

466 Mattsson, K., Ekstrand, E., Granberg, M., Hassellöv, M., Magnusson, K., 2022. Comparison
467 of pre-treatment methods and heavy density liquids to optimize microplastic extraction from
468 natural marine sediments. *Scientific Reports* 12, 15459.

469 Opfer, S., Arthur, C., Lippiatt, S., 2012. NOAA Marine Debris Shoreline Survey Field Guide.
470 U.S. Department of Commerce National Oceanic and Atmospheric Administration.

471 Rees, A. B., Turner, A., Comber, S., 2014. Metal contamination of sediment by paint peeling
472 from abandoned boats, with particular reference to lead. *Science of The Total Environment*,
473 494–495, 313–319.

474 Rubino, F., Nisticó, A., Tucci, F., Carlone, P., 2020. Marine application of fiber reinforced
475 composites: A review. *Journal of Marine Science and Engineering* 8, 26.

476 Singh, N., Turner, A., 2009. Trace metals in antifouling paint particles and their heterogeneous
477 contamination of coastal sediments. *Mar. Pollut. Bull.* 58, 559-564.

478 Song, Y.K., Hong, S.H., Jang, M., Kang, J.H., Kwon, O.Y., Han, G.M., Shim, W.J., 2014. Large
479 accumulation of micro-sized synthetic polymer particles in the sea surface microlayer.
480 *Environmental Science and Technology* 48, 9014-9021.

481 Soroldoni, S., Castro, Í.B., Abreu, F., Duarte, F.A., Choueri, R.B., Möller, O.O., Fillmann, G.,
482 Pinho, G.L.L., 2018. Antifouling paint particles: Sources, occurrence, composition and
483 dynamics. *Water Research* 137, 47-56.

484 Summerscales, J., Singh, M.M., Wittamore, K., 2016. Disposal of composite boats and other
485 marine composites. In: *Marine Applications of Advanced Fibre-Reinforced Composites*,
486 Woodhead Publishing Series in Composite Science and Engineering pp. 185-213.

487 Turner, A., Rees, A., 2016. The environmental impacts and health hazards of abandoned
488 boats in estuaries. *Regional Studies in Marine Science*, 6, 75–82.

489 Turner, A., Solman, K.R., 2016. Lead in exterior paints from the urban and suburban environs
490 of Plymouth, south west England. *Science of the Total Environment* 547, 132-136.

491 Woods, J.S., Verones, F., Jolliet, O., Vázquez-Rowe, I., Boulay, A.M., 2021. A framework for
492 the assessment of marine litter impacts in life cycle impact assessment. *Ecological Indicators*
493 12, 107918.

494

495